23-45-30

A THREE-DIMENSIONAL RIGID-LID MODEL FOR THERMAL PREDICTIONS

S. Sengupta, S. Lee, J. Venkata, C. Carter
Dept. of Mechanical Engineering
University of Miami
Coral Gables, Florida U.S.A.

ABSTRACT

A three-dimensional methematical model to predict velocities and temperature anamolies is presented. The effects of bottom topography, wind, surface heat transfer and currents are included. A co-ordinate transformation which maps variable depth basin to a constant one is used. The rigid-lid assumption is invoked. A Poissons equation is derived as the predictive equation for surface pressure. Explicit schemes are used in time to integrate the primitive conservation equations and an iterative scheme is used to solve the Poisson's equation. The model was applied to Florida Power and Light (FPL) company's fossil fuel power plant at Cutler Ridge site for April 15,1975, outfall conditons. Infra red (IR) data in the morning (0912 EST) on April 15, 1975 was used as initial conditions for temperature. The model was run for 2 hours 38 minutes and compared with IR data at (1150 EST) on the same day. The predicted results compare favorably with IR data.

NOMENCLATURE

A_H	Horizontal kinematic eddy viscosity
A_v	Vertical kinematic eddy viscosity
A_{ref}	Reference kinematic eddy viscosity
B_H	Horizontal diffusivity
B_v	Vertical diffusivity
B_{ref}	Reference diffusivity
g	Accleration due to gravity
h	Depth at any location of the basin
H	Reference depth
I	Grid index in x-direction or α direction
J	Grid index in y-direction or β direction
K	Grid index in z-direction or γ direction
K_s	Surface heat transfer coefficient
L	Horizontal length scale
P	Pressure
P_s	Surface pressure
Pr	Turbulent Prandtl number $\frac{A_{ref}}{B_{ref}}$
Pe	Peclet Number
Re	Reynolds Number
T	Temperature
T_{ref}	Reference temperature
T_E	Equilibrium temperature
t	Time
Δt	Time step used
TTOT:	Total time
u	Velocity in x-direction

v	Velocity in y-direction
w	Velocity in z-direction
x	Horizontal co-ordinate
y	Horizontal co-ordinate
z	Vertical co-ordinate
α	Horizontal co-ordinate in the stretched system
α_L	$= \alpha$ at I = IN
β	Horizontal co-ordinate in the stretched system
β_L	$= \beta$ at J = JN
γ	Vertical co-ordinate in the stretched system
μ	Absolute viscosity
ρ	Density
$(\bar{})$	Dimensional quantity
$(\sim)$	Dimensional mean quantity
$( )_{ref}$	Reference quantity

INTRODUCTION

A major source of thermal pollution in rivers, lakes and estuaries is the surface discharge of heated water from condensers of fossil and nuclear power plants. In order to design intake and outfall structures to avoid recirculation, sufficient knowledge of flow and temperature distribution in the receiving water near the discharge is necessary. Most of the previous work for the near field problem is of integral type. Some of the important work in integral models are that of Carter and Reiger (1974), Hoopes, Zeller and Rohlich (1971), Stolzenbach and Harleman (1973), Hirst (1972) and Stefan and Vaidyaraman (1971). Dunn, Policastro and Paddock (1975) discuss most of the integral models and their drawbacks. They also discuss numerical models, their advantages and disadvantages. Some of the numerical models for heated discharges are those of Brady and Geyer (1972), and Waldrop and Farmer (1974). All the above mentioned models both integral as well as numerical suffer some common disadvantages. These models also do not have adequate verification. The handbook prepared by Shirazi and Davis (1974) for surface discharges using formulations by Prych (1972) is the most readily usable predictive tool available at present. To date, there is no three-dimensional model which incorporates the effects of bottom topography, wind, surface heat transfer and current which has been extensively verified. These factors play an important role in the dispersion of heat. The present approach tries to incorporate all these relevant mechanisms using the divergence of Navier Stokes model developed by Sergupta and Lick (1974).

For calibration and model verification, FPL's power plant at Cutler Ridge site in Florida is considered. The objective of the present investigation was to predict velocity and temperature anamolies in the near field (i.e., the region which is most affected by the heated discharge). The region of interest is approximated to 525m along the axis of the jet and 425m across the axis of the jet. Figs. 1 and 2 show the basin and grid system.

BASIC EQUATIONS

The equations which describe the behaviour of fluid flow are those expressing the conservation of mass, momentum and energy. In order to keep the generalized nature of the model all significant terms in the conservation equations are retained. This includes the effects of buoyancy, inertia, coriolis, density and turbulent mixing. Wind shear, surface heat transfer and cross flow are also considered. The details of the derivation of the equations are presented in Sengupta and Lick (1974).

Assumptions and Approximations

The rigid-lid approximation is made. The rigid-lid approximation is that a rigid wall is placed on the top which allows horizontal velocities, but forces vertical velocities at the surface to zero. This approximation was used by Bryan (1969) Sengupta and Lick (1974) and several others.

This approximation is permissible as it eliminates surface gravity waves and are thereby associated instabilities. This approximation allows use of larger time steps thus saving computer time.

Since the velocities are small, the vertical momentum equation is replaced by the hydrostatic approximiation.

Turbulence is modelled using eddy transport coefficients. Constant, but different values are used for horizontal and vertical directions. The eddy transport coefficients are found by trial and error method till the correct values are obtained.

In order to overcome programming difficulties the equations are stretched vertically using the transformation,

$$\gamma = z / h(x,y)$$

Now the equations will be transformed from (x,y,z) coordinate system to a more convenient coordinate system (x,y,γ) or for convenience (α,β,γ). The advantage of this transformation is that the same number of grid points can be used in the vertical direction at shallow as well as deeper parts. Now the equations after using the above transformation will take the form shown below:

continuity

$$\frac{\partial(hu)}{\partial\alpha} + \frac{\partial(hv)}{\partial\beta} + \frac{\partial\Omega}{\partial\gamma} = 0 \tag{1}$$

momentum-u

$$\frac{\partial(hu)}{\partial t} + \frac{\partial(huu)}{\partial\alpha} + \frac{\partial(huv)}{\partial\beta} + h\frac{\partial(\Omega u)}{\partial\gamma} - \frac{h}{R_B}v = -h\frac{\partial Ps}{\partial\alpha}$$

$$- hB_x + \frac{1}{Re}\frac{\partial}{\partial\alpha}\left(h\frac{\partial u}{\partial\alpha}\right) + \frac{1}{Re}\frac{\partial}{\partial\beta}\left(h\frac{\partial u}{\partial\beta}\right) + \frac{1}{\epsilon^2 Re}\frac{1}{h}\frac{\partial}{\partial\gamma}\left(A_v^* \frac{\partial u}{\partial\gamma}\right) \tag{2}$$

momentum-v

$$\frac{\partial(hv)}{\partial t} + \frac{\partial(huv)}{\partial\alpha} + \frac{\partial(hvv)}{\partial\beta} + h\frac{\partial(\Omega v)}{\partial\gamma} + \frac{h}{R_B}u = -h\frac{\partial Ps}{\partial\beta}$$

$$-hB_y + \frac{1}{Re}\frac{\partial}{\partial\alpha}\left(h\frac{\partial v}{\partial\alpha}\right) + \frac{1}{Re}\frac{\partial}{\partial\beta}\left(h\frac{\partial v}{\partial\beta}\right) + \frac{1}{\epsilon^2 Re}\frac{1}{h}\frac{\partial}{\partial\gamma}\left(A_v^* \frac{\partial v}{\partial\gamma}\right) \tag{3}$$

hydrostatic equation

$$\frac{\partial p}{\partial\gamma} = Eu\,(1+\rho)\,h \tag{4}$$

energy

$$\frac{\partial(hT)}{\partial t} + \frac{\partial(huT)}{\partial\alpha} + \frac{\partial(hvT)}{\partial\beta} + h\frac{\partial(\Omega T)}{\partial\gamma} = \frac{1}{Pe}\frac{\partial}{\partial\alpha}\left(h\frac{\partial T}{\partial\alpha}\right)$$

$$+ \frac{1}{Pe}\frac{\partial}{\partial\beta}\left(h\frac{\partial T}{\partial\beta}\right) + \frac{1}{Pe\,\epsilon^2}\frac{1}{h}\frac{\partial}{\partial\gamma}\left(B_v^* \frac{\partial T}{\partial z}\right) \tag{5}$$

Eq of state

$$\rho = f'(T) \tag{6}$$

Poisson equation

$$\frac{\partial^2 Ps}{\partial\alpha^2} + \frac{\partial^2 Ps}{\partial\beta^2} = \frac{1}{h}\frac{\partial}{\partial\alpha}\left(-Ax_1 + Ax_2 + Cx - x_p\right) + \frac{1}{h}\frac{\partial}{\partial\beta}\left(-Ay_1 -\right.$$

$$\left. Ay_2 + Cy - Y_p\right) - \frac{1}{h}\left\{\frac{\partial h}{\partial\alpha}\frac{\partial Ps}{\partial\alpha} + \frac{\partial h}{\partial\beta}\frac{\partial Ps}{\partial\beta}\right\} - \frac{\partial(\Omega)}{\partial t}(z = 0) \tag{7}$$

where

$$u = \tilde{u}/Uref; \quad v = \tilde{v}/U_{ref}; \quad w = \tilde{w}/U_{ref}; \quad t = \tilde{t}/t_{ref}$$

$$x = \tilde{x}/L; \quad y = \tilde{y}/L; \quad z = \tilde{z}/H; \quad \epsilon = H/L$$

$$P = \tilde{P}/\rho_{ref}U^2_{ref}; \quad T = \frac{\tilde{T}-Tref}{T_{ref}}; \quad \rho = \frac{\tilde{\rho}-\rho_{ref}}{\rho_{ref}}$$

$$A^*_H = A_H/A_{ref}; \quad A^*_V = A_V/A_{ref}; \quad B^*_H = B_H/B_{ref}; \quad B^*_V = B_V/B_{ref}$$

$$t_{ref} = L/U_{ref}$$

$$Re = \frac{U_{ref}L}{A_{ref}}; \quad R_B = \frac{U_{ref}}{fL}; \quad Pr = \frac{A_{ref}}{B_{ref}}$$

$$Pe = Re \cdot Pr = \frac{U_{ref}L}{B_{ref}}; \quad Eu = \frac{gH}{U^2_{ref}}$$

In all the above terms "ref" stands for reference quantities, H and L are vertical and horizontal length scales. The variables with wavy lines on top are dimensional quantities. If A_H = Aref and B_H = B ref then $A^*_H = B^*_H = 1$. If Pr = 1 then $A_{ref} = B_{ref}$

and

$$B_x = Eu\frac{\partial h}{\partial \alpha}\int_o^\gamma \rho\, d\gamma + Euh\frac{\partial}{\partial \alpha}\int_o^\gamma \rho\, d\gamma - Eu\gamma\frac{\partial h}{\partial \alpha}\rho$$

$$B_y = Eu\frac{\partial h}{\partial \beta}\int_o^\gamma \rho\, d\gamma + Euh\frac{\partial}{\partial \beta}\int_o^\gamma \rho\, d\gamma - Eu\gamma\frac{\partial h}{\partial \beta}\rho$$

$$\tilde{w} = \gamma\left(\tilde{u}\frac{\partial \tilde{h}}{\partial x} + \tilde{v}\frac{\partial \tilde{h}}{\partial Y}\right) + \tilde{h}\,\tilde{\Omega}$$

$$\Omega = \frac{\partial \gamma}{\partial \tilde{t}}$$

$$A_{X_1} = \int_o^1 \left\{\frac{\partial}{\partial \alpha}(huu) + \frac{\partial}{\partial \beta}(huv) + h\frac{\partial}{\partial \gamma}(\Omega u)\right\} d\gamma$$

$$A_{X_2} = \frac{h}{R_B} \int_o^1 v\,d\gamma$$

$$C_X = \frac{1}{Re} \int_o^1 \left\{ \frac{\partial}{\partial\alpha} \left(h \frac{\partial u}{\partial\alpha}\right) + \frac{\partial}{\partial\beta} \left(h \frac{\partial u}{\partial\beta}\right) + \frac{1}{\epsilon^2 h} \frac{\partial}{\partial\gamma} \left(A_V^* \frac{\partial u}{\partial_\gamma}\right) \right\} d\gamma$$

$$X_p = Eu \int_o^1 h \left\{ \frac{\partial h}{\partial X} \int_o^\gamma \rho\,d\gamma + h \frac{\partial}{\partial\alpha} \int_o^\gamma \rho\,d\gamma - \gamma \frac{\partial h}{\partial\alpha} \rho \right\} d\gamma$$

$$A_{y_1} = \int_o^1 \left\{ \frac{\partial}{\partial\alpha} (huv) + \frac{\partial}{\partial\beta} (hvv) + h \frac{\partial(\Omega v)}{\partial\gamma} \right\} d\gamma$$

$$A_{y_2} = \frac{h}{R_B} \int_o^1 u\,d\gamma$$

$$C_y = \frac{1}{Re} \int_o^1 \left\{ \frac{\partial}{\partial\alpha} \left(h \frac{\partial v}{\partial\alpha}\right) + \frac{\partial}{\partial\beta} \left(h \frac{\partial v}{\partial\beta}\right) + \frac{1}{\epsilon^2 h} \frac{\partial}{\partial\gamma} \left(A_V^* \frac{\partial v}{\partial\gamma}\right) \right\} d\gamma$$

$$Y_p = Eu \int_o^1 h \left\{ \frac{\partial h}{\partial\beta} \int_o^\gamma \rho\,d\gamma + h \frac{\partial}{\partial\beta} \int_o^\gamma \rho\,d\gamma - \gamma \frac{\partial h}{\partial\beta} \rho \right\} d\gamma$$

The last term in equation (7) is the Hirt and Harlow (1967) correction term. This term is not set equal to zero even though the rigid-lid conditions imply W (Z = 0) = 0. This is in anticipation of the errors which will arise when the Poisson equation is solved by iterative technique. If these errors are not corrected, the continuity equation will not be satisfied leading to accumulation or loss of fluid from the system.

Equations 1 through 7 form the set of equations which are to be solved with appropriate boundary conditions.

Boundary Conditions

The boundary conditions used are shown in Fig. 3. The conditions on solid walls and bottom are no slip and no normal velocity for all time for the momentum equations, except $W \neq 0$ at side wall due to hydrostatic approximation. The temperature boundary condition at solid walls and bottom is handled by assuming the walls and bottom adiabatic. The boundary condition for velocity and temperature at open boundaries is $\frac{\partial f}{\partial n} = 0$, where $\frac{\partial f}{\partial n}$ is velocity or temperature gradient normal to the boundary. At the air-water interface the boundary condition on the momentum equations are obtained in the form of wind stress. The temperature boundary condition at the air water interface due to Edinger & Geyer (1971) is

$$\text{Heat flux} = \Delta Q = K_s \, (\tilde{T}_E - \tilde{T}_S)$$

where K_S is surface heat transfer coefficient and T_E and T_S are equilibrium and surface temperatures. The boundary conditions for the Poisson equation are Neuman type along solid boundary and along open boundaries the pressure is assumed constant.

The boundary conditions in summary for the stretched system of equations are:

Along the shore:

$$u = 0$$

$$v = 0$$

$$\Omega \neq 0$$

$$\frac{\partial T}{\partial Y} = \frac{\partial T}{\partial \beta} - \frac{\gamma}{h} \frac{\partial h}{\partial \beta} \frac{\partial T}{\partial \gamma} = 0$$

At the bottom of the basin (γ=1):

$$\Omega = 0$$

$$u = 0$$

$$v = 0$$

$$\frac{\partial T}{\partial \gamma} = 0$$

Along free boundaries:

At $(\alpha = 0, \beta, \gamma)$

$U_{I=1,\ K} = U_{I=2,K}$

$v = 0$

$w \neq 0$

$T_{I=1,\ K} = T_{I=2,\ K}$

P_s = constant

At $(\alpha = \alpha_L,\ \beta, K)$

$U_{I=IN,\ K} = U_{I=IN-1,\ K}$

$v = 0$

$w \neq 0$

$T_{I=IN,\ K} = T_{I=IN-1,\ K}$

P_s = constant

At $(\alpha, \beta = \beta_L,\ \gamma)$

$V_{JN,\ K} = V_{JN-1,\ K}$

$u = 0$

$w \neq 0$

P_s = constant

At inflow boundaries, the velocity of current is specified

At the air-water interface

$\Omega = 0$ (Rigid-lid)

$$\frac{\partial u}{\partial \gamma} = \left(\frac{hH}{U_{ref} A_V}\right) \tau_{zx}$$

$$\frac{\partial v}{\partial \gamma} = \left(\frac{hH}{U_{ref} A_V}\right) \tau_{zy}$$

$$\frac{\partial T}{\partial \gamma} = \left(\frac{hHK_s}{B_z}\right) (T_E - T_s)$$

ARRANGEMENT OF VARIABLES AND GRID SYSTEM

The grid system and arrangement of variables are shown in Fig. 4. u and v are located on integral nodes (I,J,K) on the horizontal (x,y) plane. P,T,W,ρ are located at half grid points (I + ½, J + ½, k). This arrangement is repeated in Z direction. This kind of arrangement allows better meshing of the variables without calculating all variables at all nodes of the staggered mesh system. Constant grid spacing is used in σ or Z direction. Constant grid spacing is also used in x and y (or α and β) directions.

METHOD OF SOLUTION

The method of solution is explicit using forward time central space (FTCS) schemes except in the diffusion term. The diffusion terms are differenced by the Dufort-Frankel scheme. The initial values of variables are specified and then the equations are integrated marching in time. The only iterative procedure involves the solution of the equation for surface pressure.

Since it is not possible to make a strict stability analysis for the system of equation under consideration, one-dimensional Burgers equation is used for stability analysis.

The stability cirıterion for the equations under consideration is therefore:

<u>convective criterion</u>

$$u \frac{\Delta \bar{t}}{\Delta \tilde{x}} + v \frac{\Delta \bar{t}}{\Delta \tilde{y}} + w \frac{\Delta \bar{t}}{\Delta \tilde{Z}} \leq 1$$

<u>diffusion</u>

$$A_H \frac{\Delta \bar{t}}{(\Delta \tilde{x})^2} + A_H \frac{\Delta \bar{t}}{(\Delta \tilde{y})^2} + A_V \frac{\Delta \bar{t}}{(\Delta \tilde{Z})^2} \leq \frac{1}{2}$$

$$B_H \frac{\Delta\bar{t}}{(\Delta\tilde{x})^2} + B_H \frac{\Delta\bar{t}}{(\Delta\tilde{y})^2} + B_V \frac{\Delta\bar{t}}{(\Delta\tilde{z})^2} \leq \tfrac{1}{2}$$

The equations are solved on a UNIVAC/1106 computer at the University of Miami.

RESULTS

The region of influence of the Cutler Ridge plume has been approximated to a rectangular domain as shown in Fig. 1. It extends 425 meters in lateral extent and 525 meters in longitudinal extent. The discharge is taken as 25 meters wide. The numerical grid system is shown in Fig. 2. It has 18 and 22 nodes across and along the axis of the jet respectively. There are 5 nodes in the vertical direction.

In order to understand the physical processes involved and to investigate the numerical behaviour of the model several simplified cases were executed before the final calibration and verification run for April 15,1975.

Case 1

This case was designed to study the effects of bottom topography. A section of bottom topography can be seen in Fig. 5. The topography is symmetrical about the discharge centerline. The canal is 6 meters deep gradually merging into the bay which is 1.2 meters deep. The steady state surface velocities are symmetrical as expected, since the effects of wind and current are neglected and the bottom topography is symmetrical about the centerline. These results are shown in Fig. 6. There is a reduction in velocities in the bottom layers owing to bottom shear. Fig. 5 shows centerline surface velocity with distance from discharge origin at different times. The steady state curve (155 min) shows that the velocity decays to about 75 meters and then gradually increases to a value slightly higher than the initial discharge velocity at a distance of 175 meters. The reason for this is that the depth is initially constant along the jet and the velocity decays as expected. However, after 75 meters the depth decreases linearly to 1.2 meters in the next 75 meters thus causing a constricting effect which increases the velocity offsetting the decrease caused by lateral mixing. Here again it can be seen that the time to reach steady state increases with distance from the jet origin.

Case 2

The effects of density variations is studied in this case. The basin was taken as constant depth 1.2 meters and effects of wind and current neglected. The discharge temperature is 35.9°C and the ambient temperature is 28.0°C. Fig. 7 shows the surface isotherms. The inertial core of the discharge can be seen as an elongated wedge of warm water at the mouth of the discharge. The isotherms are symmetrical as expected, since the effects of wind and current are neglected. The centerline temperature decay of the plume is shown in Fig. 8. The behaviour is very similar to the surface velocity decay. This is because the dispersal of heat and momentum essentially have the same mechanisms. The temperature decay near the origin is therefore followed by a region of rapid decay caused by entrainment. Finally as the difference in temperature is reduced the temperature asymptotically approaches the ambient value.

Case 3

This case includes the effects of strong wind along with density variations on a discharged plume into a constant depth basin. The wind was blowing at 6.71 m/sec (15 mph) 160°N. Fig. 9 shows surface velocities. The wind driven current is very dominant for most of the flow. The effect of wind slowly reduced in the bottom layers, finally being dominated by bottom shear near the floor of the basin. Fig. 10 shows the skewed plume. The plume is turned towards the west. The skewing increases with time until a steady state is reached.

Case 4

The data base for this case is obtained from the field experiments conducted at the Cutler Ridge site on April 15, 1975. The initial temperature conditions are taken from the morning IR data (0911-0912 EST) and ground truth data on April 15,1975. The computations were continued for 2 hrs. 38 min. Fig. 11 shows isotherms predicted by the model along with IR data (11:45-11:55 EST) on April 15,1975. As can be seen there is reasonably good agreement between IR data and model predicted results. Fig. 12 shows temperature decay along J at I=11 (close to centerline) predicted by the model along with IR data. There is a good agreement between IR data and model results. The isotherms along I and J sections are shown in Figs. 13 and 14 respectively.

TABLE 1

CASE NO.	DEPTH	DENSITY	WIND STRESS (WIND SPEED)	CURRENT	REMARKS
1	Variable	Constant	None	None	Steady State (TTOT = 155 min) Δt = 30 sec.
2	Constant (1.2 m)	Variable	None	None	TTOT = 1/2 hr. Δt = 15 sec.
3	Constant (1.2 m)	Variable	15 mph 6.71 m/sec	None	TTOT = 2 1/2 hrs. Δt = 15 sec
4	Constant (1.2 m)	Variable	15 mph 6.71 m/sec	3 cm/sec south	TTOT = 2 hrs. 38 min. Δt = 10 sec.

The following values are used in the above cases:

Discharge Vel : 20 cm/sec K_S = 100 BTU/^{o}F-Ft^2-day

Discharge Temp: 35.9^{o}C

Initial Temp : 28.0^{o}C

Air Temp : 29.5^{o}C

Case 4 is ran with IR data initial conditions

Stratification near discharge with isothermal conditions away from the plume can be seen in Fig. 13.

SUMMARY

Simple cases have been investigated to obtain an understanding of the basic mechanisms of the behaviour of a buoyant surface jet. Effects of wind, topography and current have been documented. Comparison with data bases obtained for field measurements, (both in-situ and airborne IR) is good. The model can be used either for preparation of environmental impact satements or research in buoyant surface jets.

ACKNOWLEDGEMENTS

The authors wish to thank National Aeronautics and Space Administration, Kennedy Space Center, for the financial assistance provided under contract NASA10-8740. NASA-KSC personnel were also responsible for providing remote sensing support.

REFERENCES

1. Brady, D. and Geyer, J., "Development of General Computer Model for Simulating Thermal Discharges in Three-Dimensions", Report No. 7, Dept. of Geography and Environmental Eng., Johns Hopkins University, Baltimore, Md. (1972).

2. Bryan,K., "A Numerical Method for the Study of the World Oceans", Journal of Computational Physics, Vol. 4, 1969.

3. Carter, H.H. and Reiger, R., "The three-dimensional Heated Surface jet in a Cross Flow", Technical Report 88, Chesapeake Bay Institute, Johns Hopkins University, Baltimore, Md. (1974).

4. Dunn, W.E., Policastro, A.J., and Paddock, R.A., "Surface Thermal Plumes: Evaluation of Mathematical Models for the Near and Complete Field", Water Resources Research Program, Energy and Environmental Systems Division, Argonne National Laboratory, Argonne, Illinois (Part one and two) (1975).

5. Edinger, J.E. and Geyer, J.C., "Heat Exchange in the Environment", E.E.I. publication, No. 65-902, Edison Electric Institute, 1971.

6. Hirst, E., "Buoyant Jets with Three-Dimensional Trajectories", Journal of Hydraulics Division, ASCE, Vol. 98, Nov.,

1972, pp 1999-2014.

7. Hirt, C.W. and Harlow, F.W., "A General Corrective Procedure for the Numerical Solution of Initial Value Problems", Journal of Computational Physics, Vol. 2, 1967.

8. Hoopes, J.A., Zeller, R.W., and Rohlich, G.A., "Heated Surface Jets in a Steady Crosscurrent", Journal of Hydraulic Div., ASCE, Vol. 97, Sept. 1971, pp 1403-1426.

9. Prych, E., "A Warm Water Effluent Analyzed as A Buoyant Surface Jet", Swedish Meteorological and Hydrological Inst., Hydraulic Series No. 21 (1972).

10. Sengupta, S. and Lick, W.J., "A Numerical Model for Wind Driven Circulation and Temperature Fields in Lakes and Ponds, FTAS/TR-74-99, Case Western Reserve University, 1974.

11. Shirazi, M. and Davis, L., AWorkbook of Thermal Plume Prediction", Vol. 2, Surface Discharge Pacific Northwest Environmental Research Laboratory Report EPA-R2-72-0056, Corvallis, Oregon, (May,1974).

12. Stefan,H., and Vaidyaraman,P., "Jet-Type Model for the Three-Dimensional Thermal Plumes in a Crosscurrent and Under Wind", Water Resources Research, Vol. 2, No. 4 (Aug.,1972) pp 998-1014.

13. Stolzenbach, K., and Harleman,D., "Three-Dimensional Heated Surface Jets', Water Resources Research Vol. 9, No. 1 (Feb.,1973).

14. Waldrop, W.R. and Farmer, R.C., "Three-Dimensional Computation of Buoyant Plumes", Journal of Geophysical Research, Vol. 79, No. 9 (March,1974).

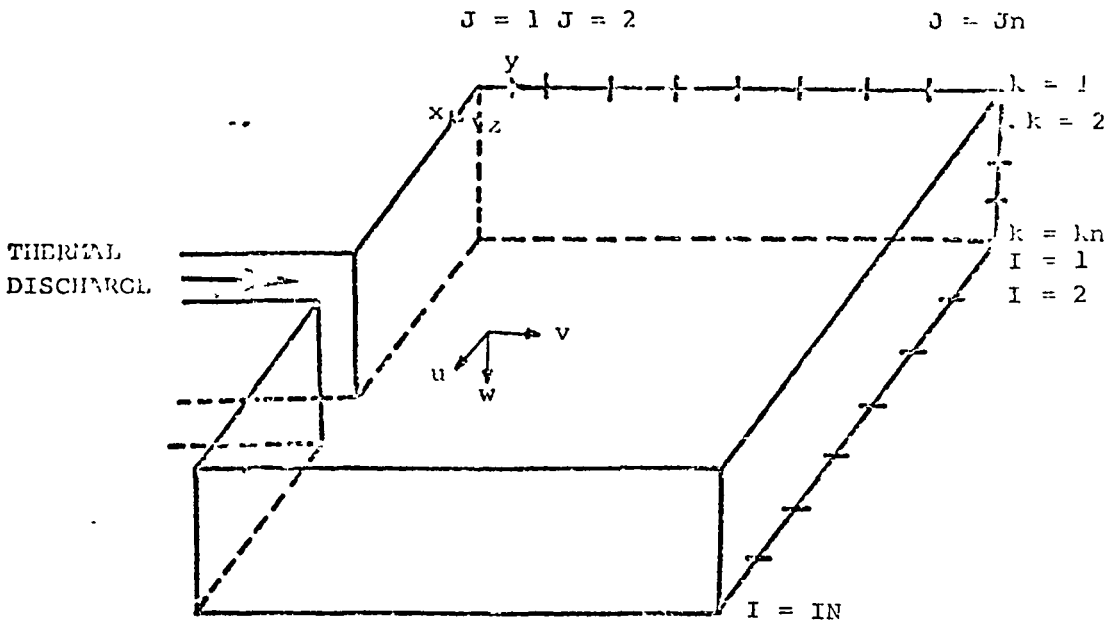

Fig. 1 Coordinate and Grid System

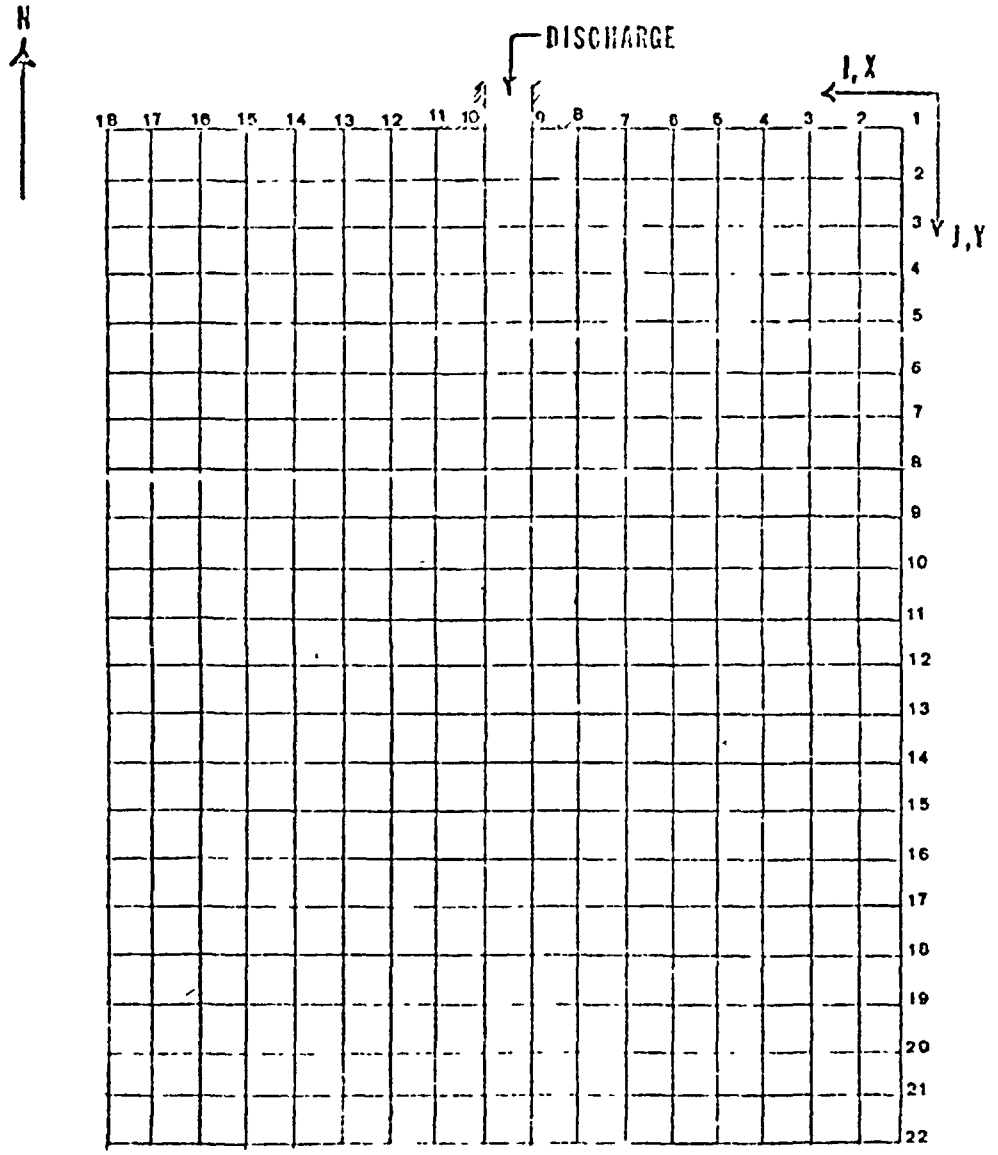

Fig. 2 Grid System For Rigid-Lid Near Field Model of Cutler Ridge Site

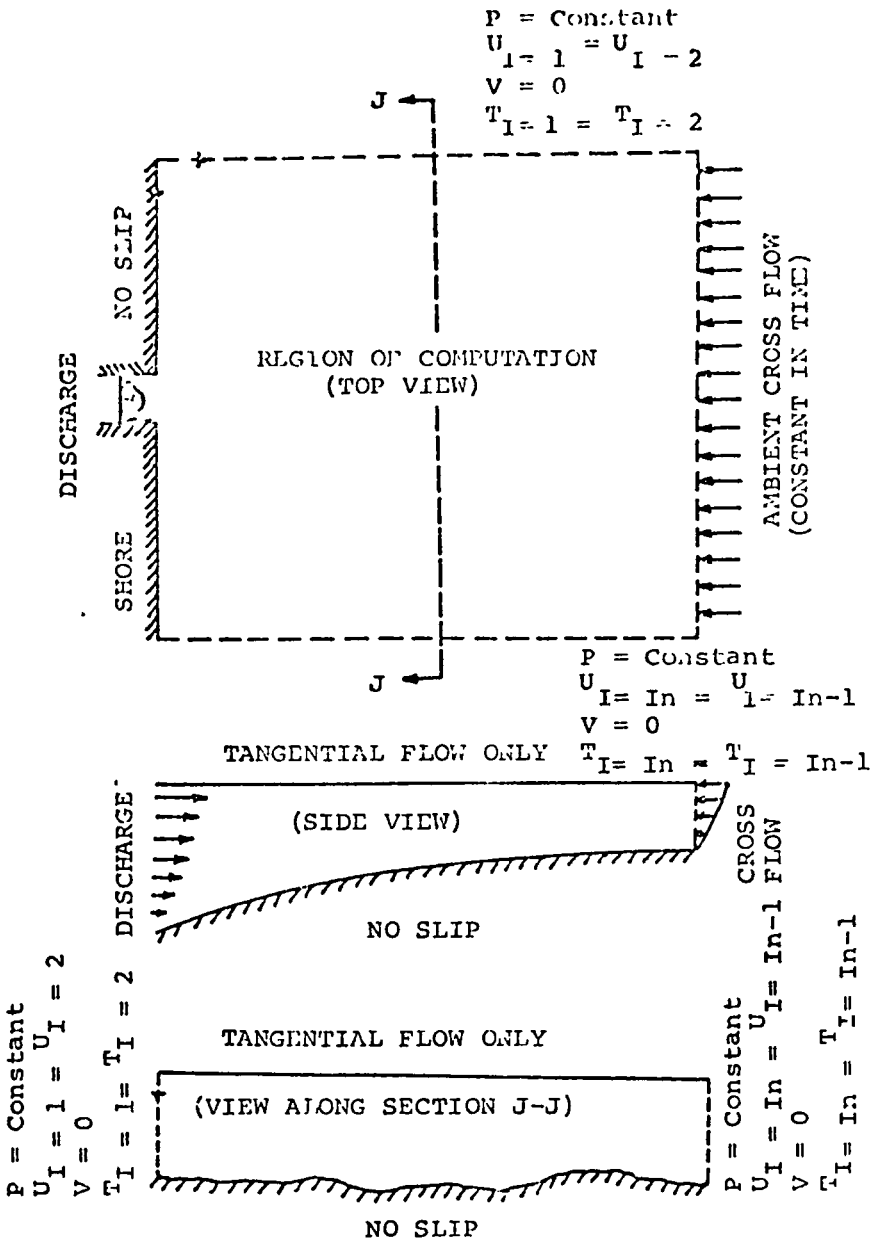

Fig. 3. Boundary Conditions for the Region of Computation

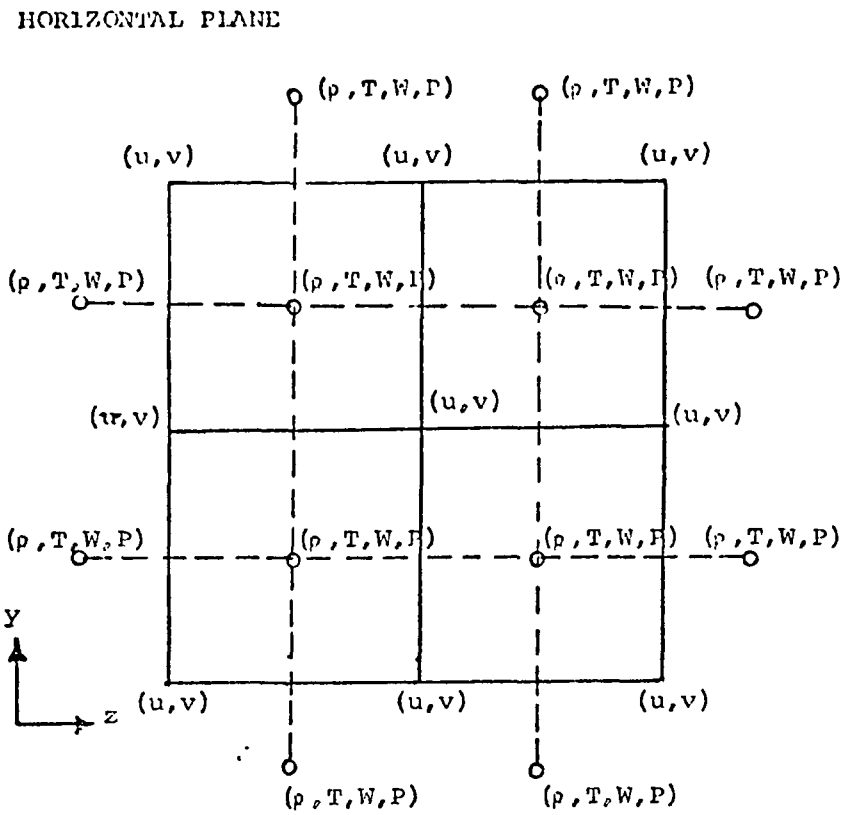

Fig. 4 Arrangement of Staggered Grid and Variables

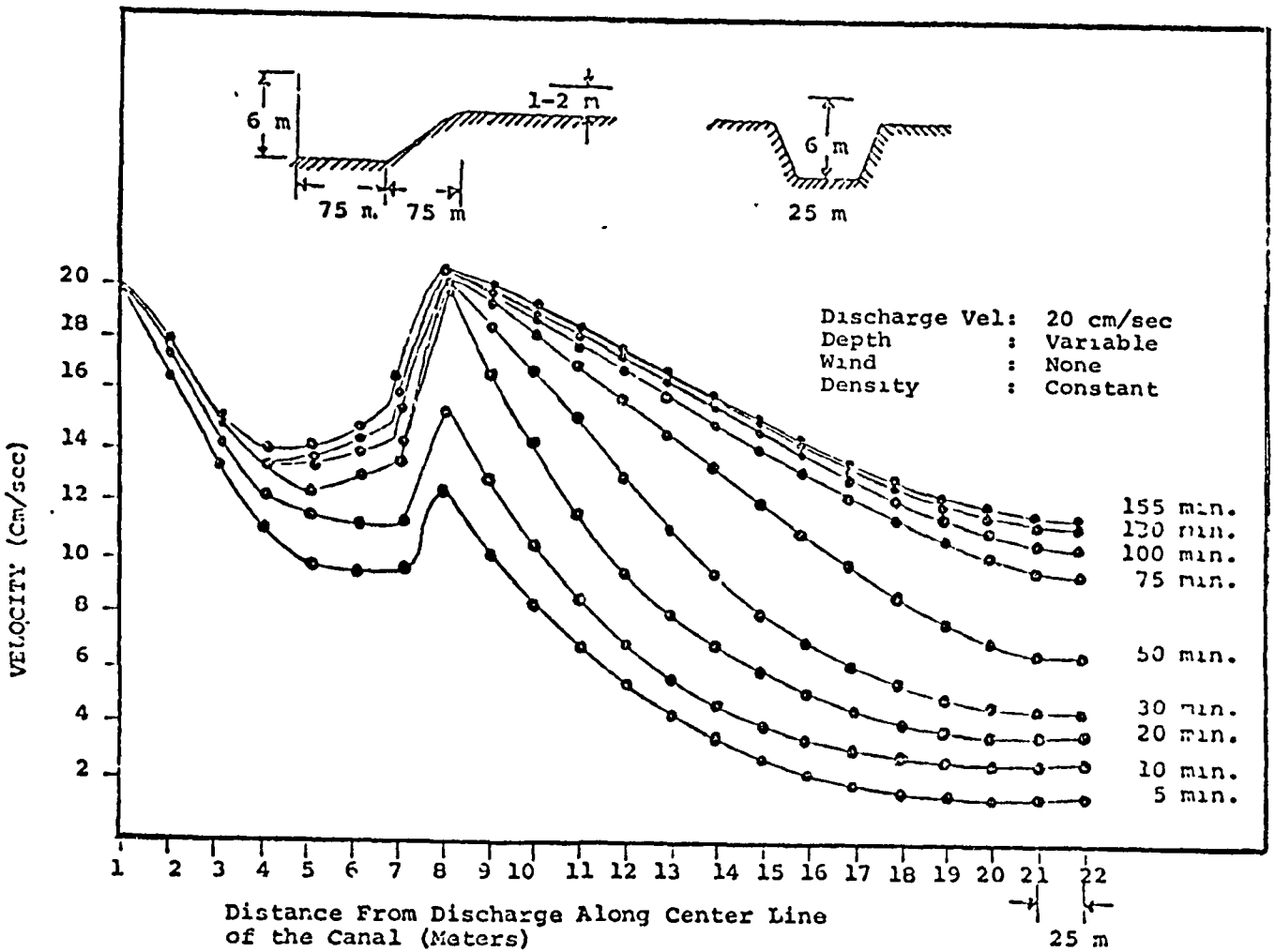

Fig. 5 Center Line Velocity Decay (Rigid-Lid Model) (Case 1)

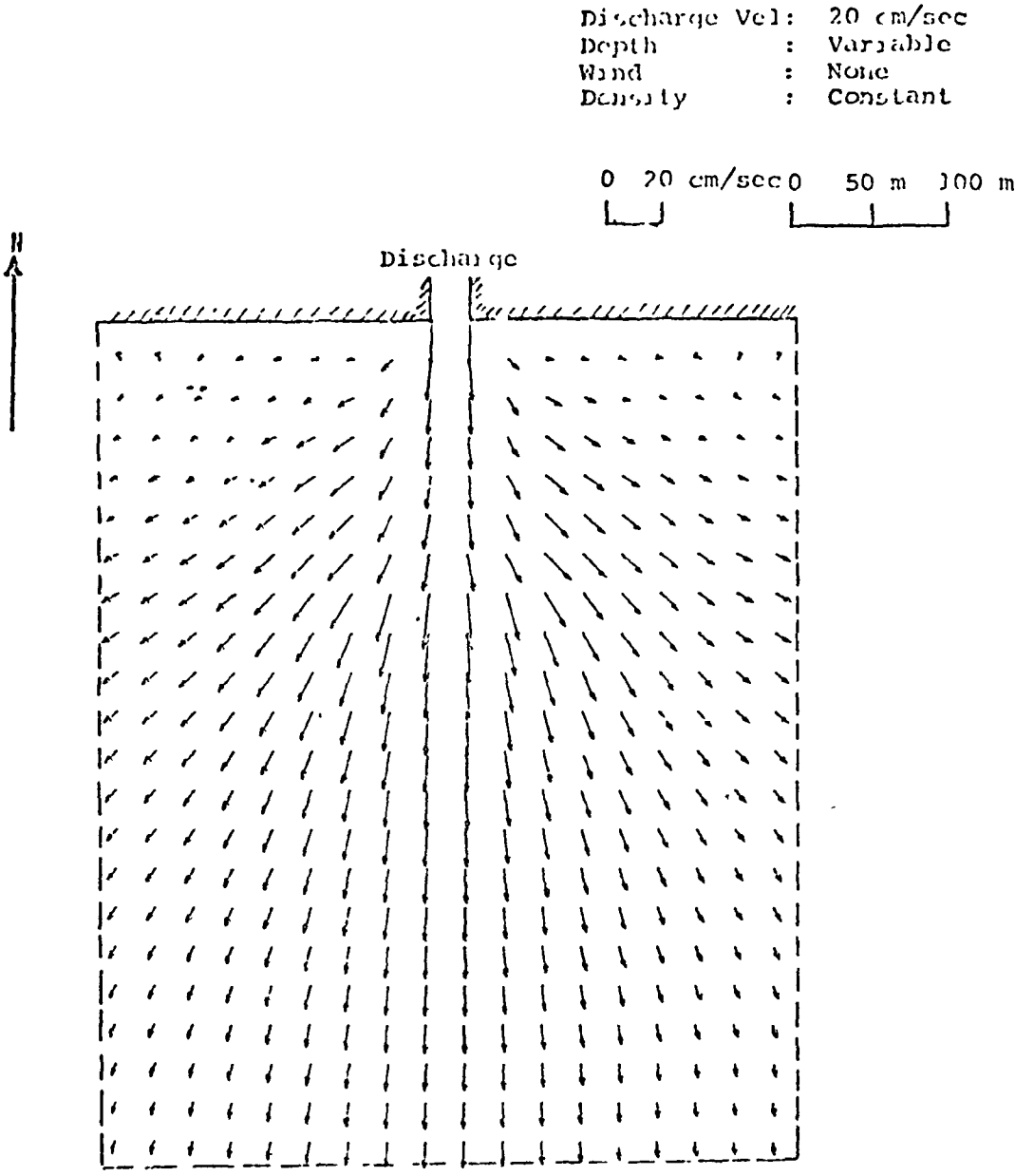

Fig. 6 Surface Velocity Distribution at Steady State For Cutler Ridge Site (Rigid-lid Model) (Case 1)

Discharge Velocity	: 20 cm/sec
Discharge Temperature	: 35.9°C
Depth	: 1.2 m
Density	: Variable
Wind	: None
T_{air}	: 29.5°C
$T_{initial}$	: 28.0°C
t_{total}	: 30 min.

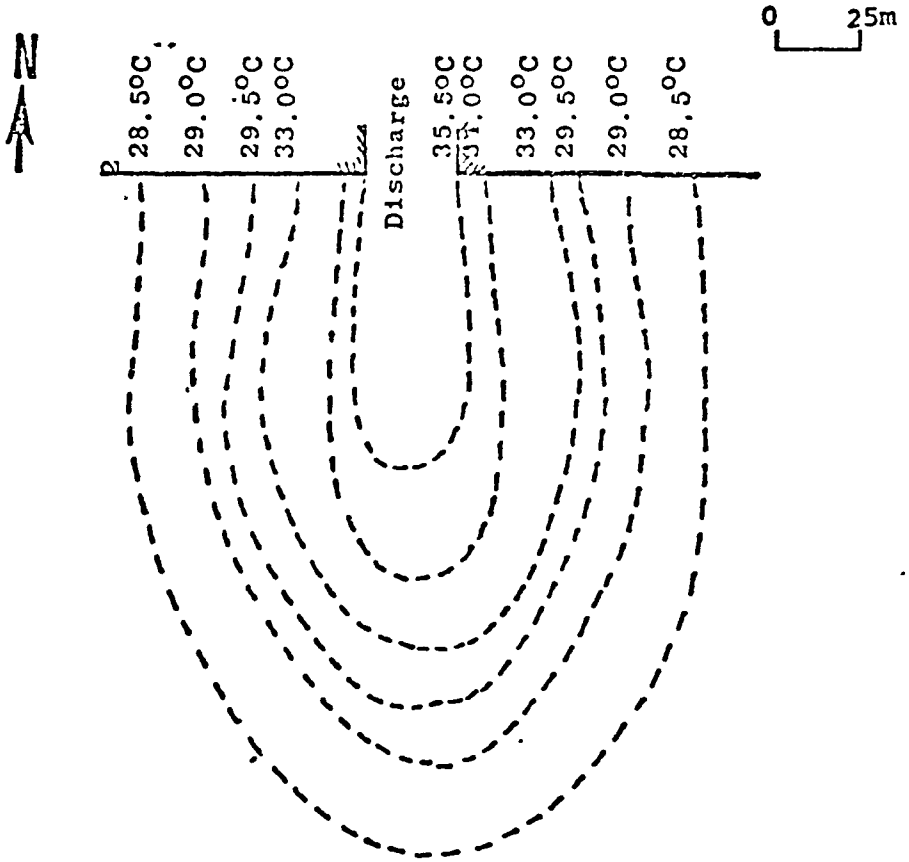

Fig. 7 Surface Isotherms for Cutler Ridge Site (Rigid-Lid) (Case 2)

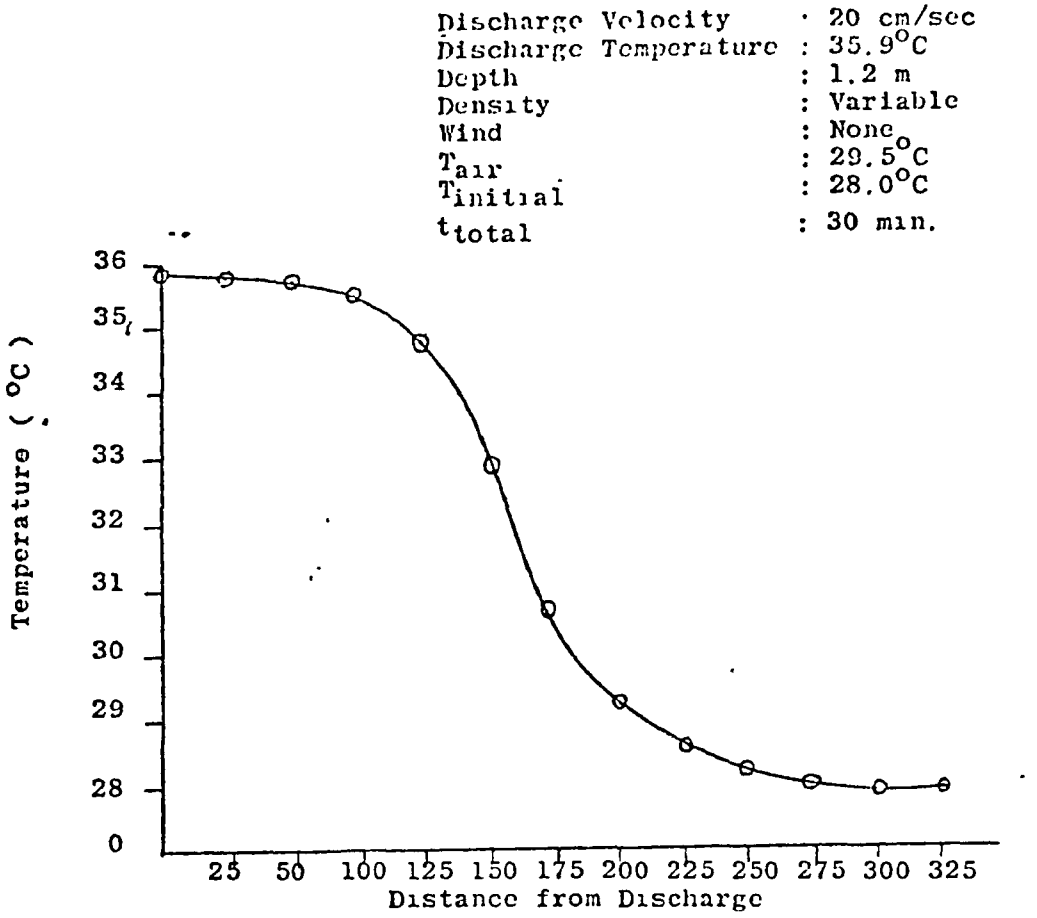

Fig. 8 Centerline Temperature Decay For Cutler Ridge Site (Rigid-Lid Model) (Case 2)

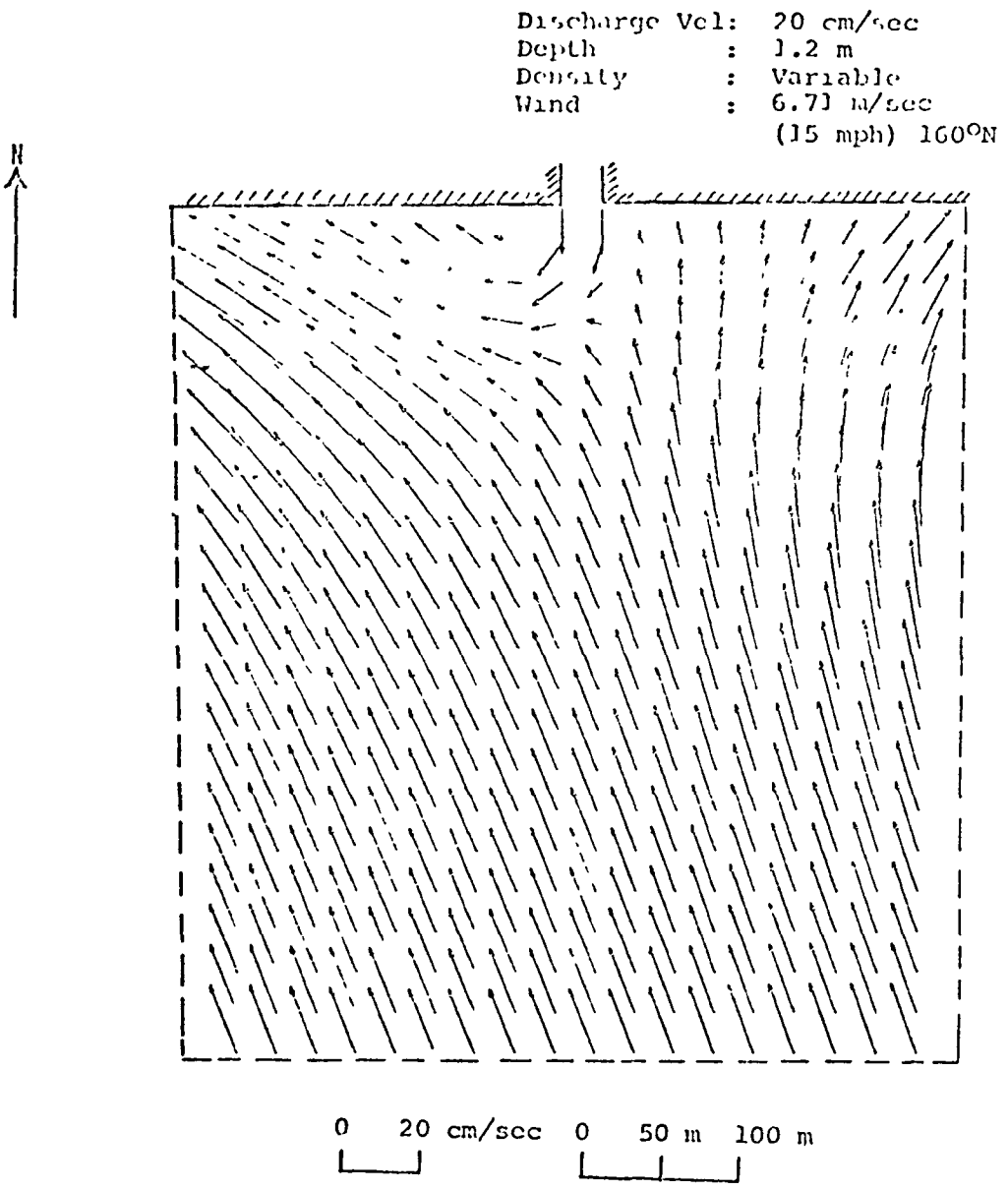

Fig. 9 Surface Velocity Distribution 2½ Hours After Discharge For Cutler Ridge Site (Rigid-Lid Model) (Case 3)

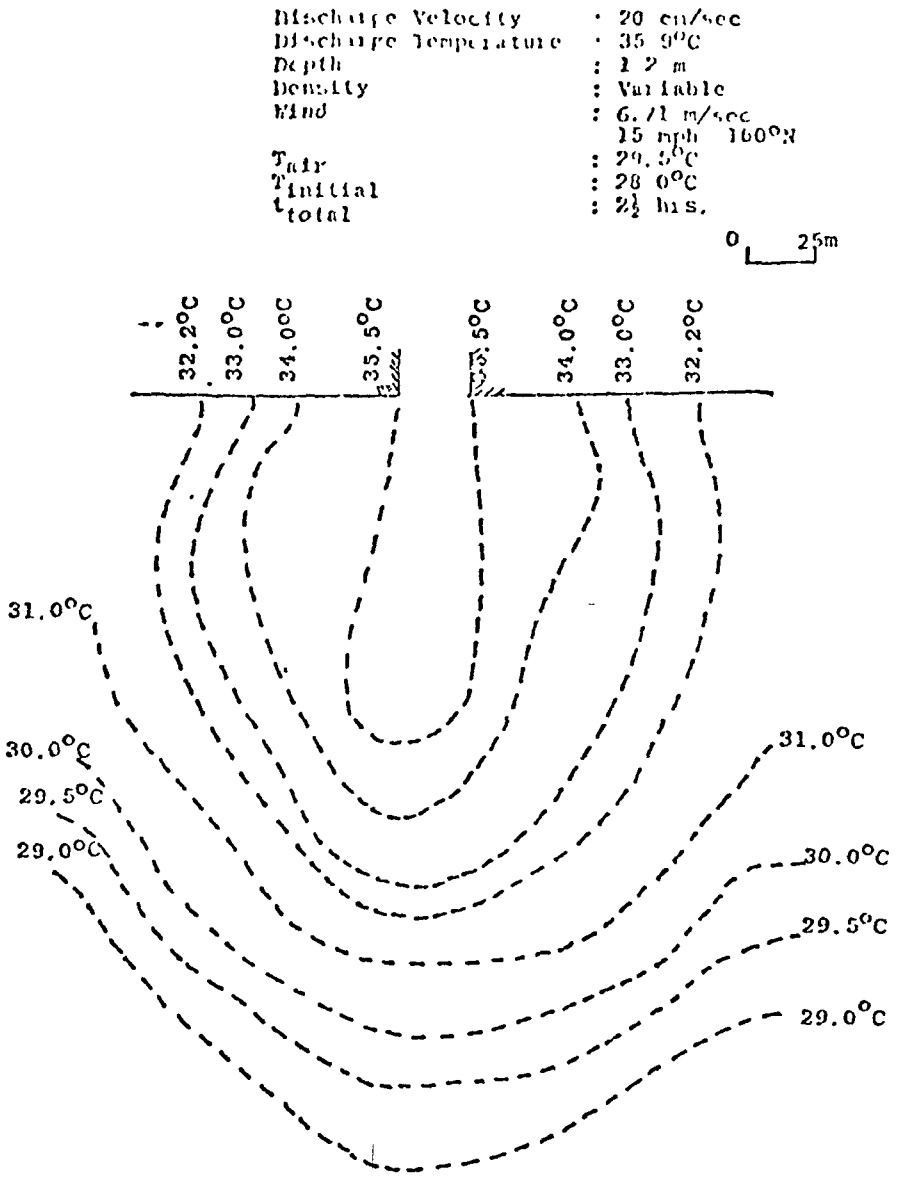

Fig. 10 Surface Isotherms for Cutler Ridge Site (Rigid-Lid) (Case 3)

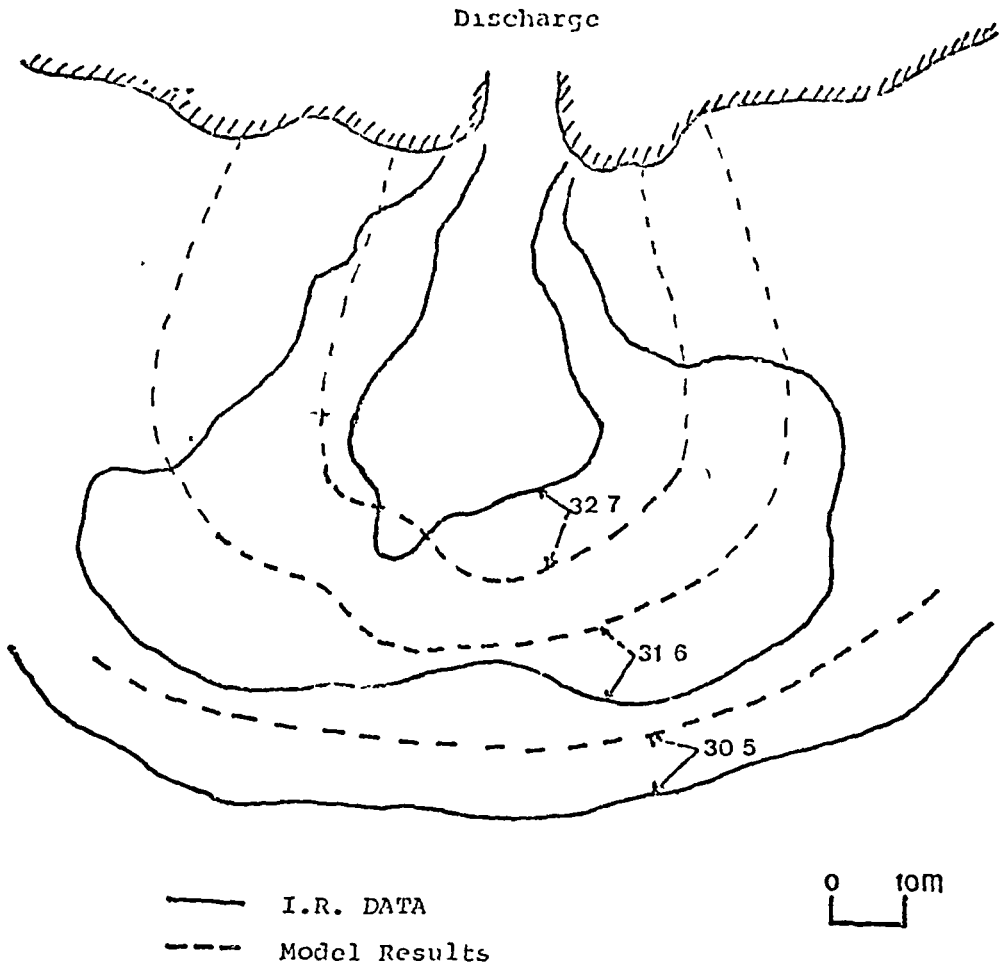

Fig. 11 Comparison of Isotherms for April 15,1975 (11:55 am) (Case 4)

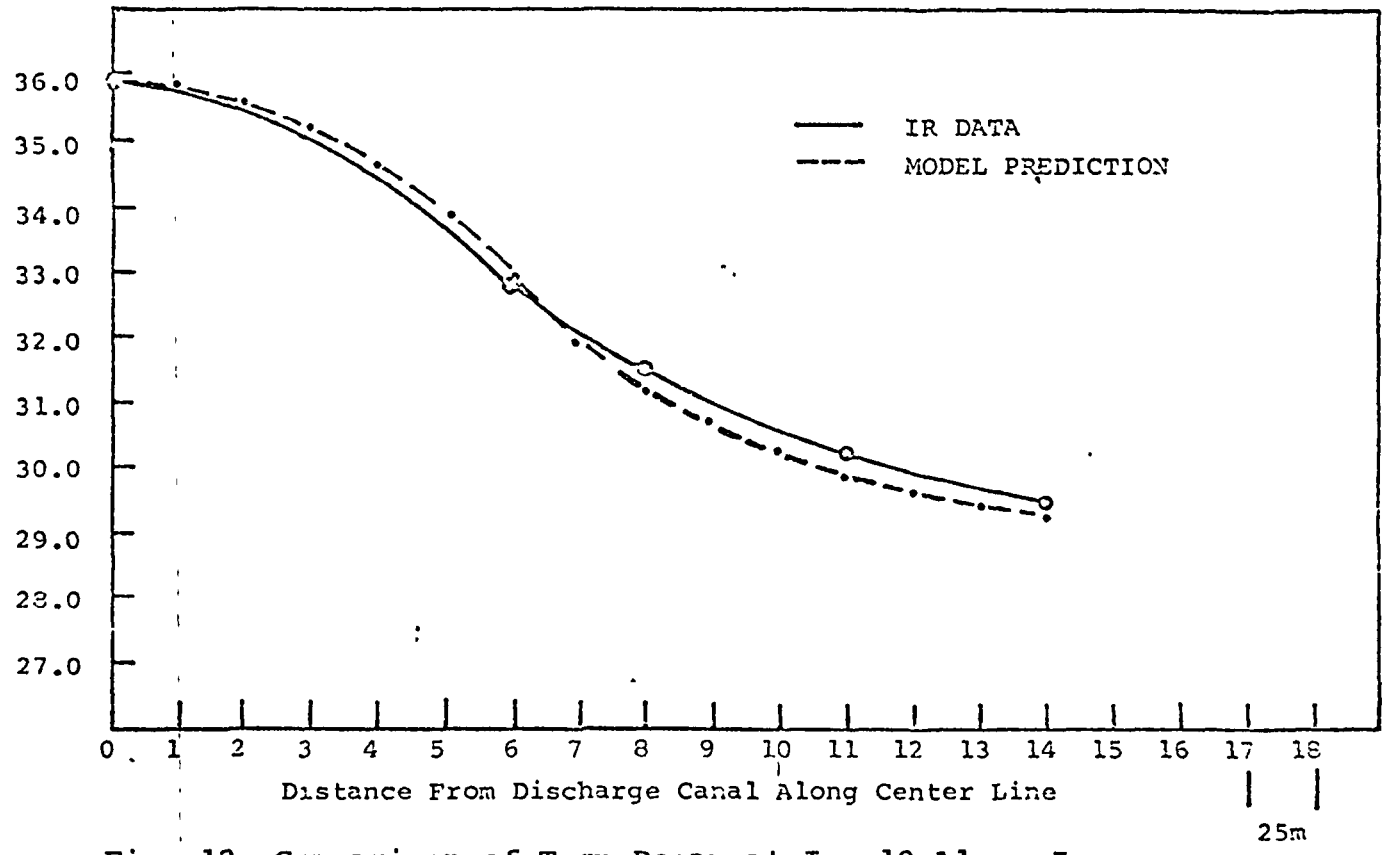

Fig. 12 Comparison of Temp Decay at I = 10 Along J (close to centerline) for April 15,1975 (11:55) (Case 4)

Date:	April 15, 1975
Discharge Vel:	20 cm/sec
Discharge T:	35.9°C
Density:	Variable
Wind:	6.71 m/sec
T air:	29.5°C
T initial:	28.0°C
Current:	3 cm/sec from South

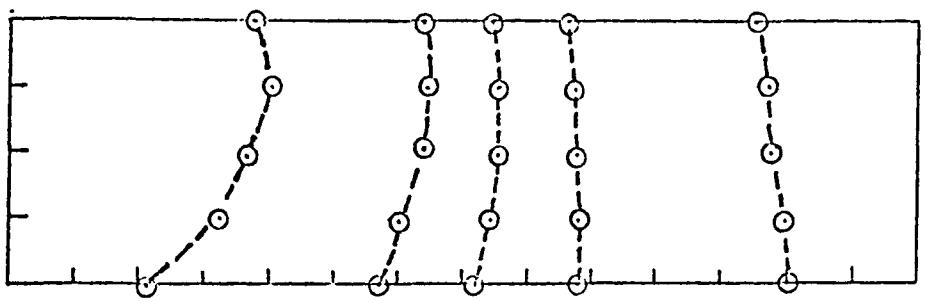

Fig. 13 Vertical Section Isotherms Along Canal Center Line for April 15,1975 at Cutler Ridge Site (Rigid-Lid) (Case 4)

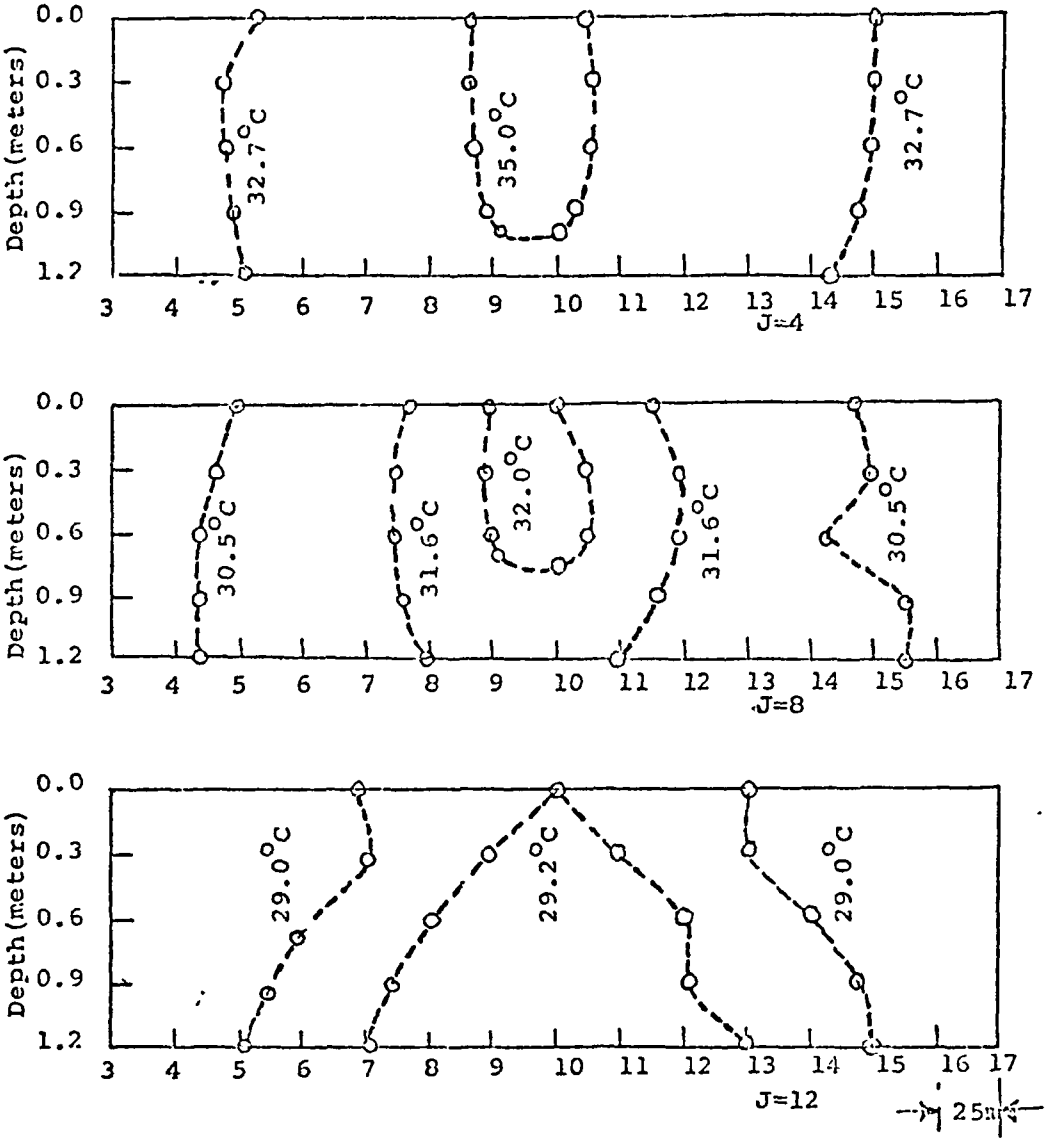

Fig. 14 Vertical Section Isotherms at Different J Sections for April 15,1975 at Cutler Ridge Site (Rigid-Lid) (Case 4)